219-6641 A

THE RESPONSE OF CaF_2:Mn THERMOLUMINESCENT DOSIMETERS TO NEUTRONS FROM A ^{252}Cf SOURCE

by

CHI-GEE KAN

B.S., National Tsing Hua University
Republic of China, 1969

A MASTER'S THESIS

submitted in partial fulfillment of the

requirements for the degree

MASTER OF SCIENCE

Department of Nuclear Engineering

KANSAS STATE UNIVERSITY
Manhattan, Kansas

1973

Approved by:

Norman Dorman J F Merklin

Major Professor

LD
2668
T4
1973
K32
c.2
Docu-
ments

TABLE OF CONTENTS

LIST OF FIGURES

LIST OF TABLES

1. INTRODUCTION

Shortly after the discovery of X rays and radioactivity toward the end of the nineteenth century, the need for measurement of energy absorbed became important not only to physicists, but also to radiologists, physicians, health physicists and others. The amount of radiation energy absorbed is known as radiation dose, and its measurement is called radiation dosimetry. The increasing use of ionizing radiation in biology, industry, medicine and other fields and the hazards involved in its use require accurate dosimetry.

One of the recently developed dosimetry techniques involves the use of radiation effects in solids. Certain types of solid materials can store energy upon irradiation and release it in the form of light at an elevated temperature. The emission of light by thermal means is called thermoluminescence, TL. The solid material used for TL for dosimetric purposes is known as a thermoluminescent dosimeter, TLD.

The TLD has been used quite widely in dosimetry due to the following properties. They are useful over a wide range of dose (10^{-4} R to 10^{8} R). They are small in size (needle shape dosimeters). They are sensitive to all kinds of ionizing radiations. They are quite accurate, reusable, convenient and easy to read out. Two main drawbacks of TLD's are the difficulty in reproduction of the phosphors due to the extreme sensitivity to minute impurity concentration and the requirement for complicated and expensive reading equipment.

A list of materials exhibiting thermoluminescence is given in ref. (1). It is seen that different characteristics of each dosimeter make it useful in some situations and not possible in others. Thermoluminescent dosimetry, utilizing the synthetic phosphor calcium fluoride manganese doped (CaF_2:Mn), was first developed by Ginther and Kirk (2) and Schulman et al. (3). CaF_2:Mn TLD's are available in two forms, TL-39 and TL-31, manufactured by EG and G company. TL-39 and TL-31 are the same in composition, but differ in size. Due to the different size, they need different read out equipment.

Although TLD can now be considered a well established technique, its fundamental theory is far from understood. All the TL techniques are empirical in nature, the dosimeters need to be calibrated before they are put in an unknown radiation field.

The primary purpose of this research is to obtain the response of CaF_2:Mn TL dosimeters to the neutrons from the ^{252}Cf source. The process is to get the calibration curves for CaF_2:Mn TLD's for gamma radiation and neutron radiation; to compare these two curves and to determine where the supralinearity (essentially non-linearity) begins, if there is any. So far, most of the efforts on the response of CaF_2:Mn TLD's has been done with gamma radiation. However considering the increasing use of CaF_2:Mn dosimetry, it is important to know the response of CaF_2:Mn to neutrons. It is hoped that this research together with other characteristics of thermoluminescence of CaF_2:Mn may contribute to our understanding of the TL mechanism.

2. THEORY

2.1 Definition of Terms

2.1.1 Radiation Absorbed Dose

2.1.1.1 Radiation Absorbed Dose in ^{252}Cf Source

Technically it is very difficult to determine the exact dose that the dosimeters absorbed in the ^{252}Cf source. The reasons are the complicated gamma rays from the fission fragments and the neutrons with a fission spectrum. In all the radiations involved in the ^{252}Cf source, the fast neutron is the dominant one. Thus the fast-neutron fluence is used as a measure of radiation absorbed dose in the ^{252}Cf source. Fluence should be an integral of flux during the irradiation interval. Since the half-life of ^{252}Cf is much longer than the period of experiment, the flux is assumed to be constant through the experiment. So, the fluence is the product of flux and irradiation time. The determination of fast-neutron flux will be discussed in Chapter 6.

2.1.1.2 Radiation Absorbed Dose in Gamma-Ray Source

In the gamma-ray source the absorbed dose unit is rad, which is defined as the absorption of 100 ergs per gram of material. The rad unit used in this study is the water rad. The absorbed rad in CaF_2:Mn is equal to the water rad times 0.8534 (4).

2.1.2 Traps

Structural imperfections can be found frequently in the crystal and form a localized center for positive or negative charge. When the radiation is absorbed, electrons and holes are created due to ionization and can be trapped by localized centers. After thermal excitation the trapped electrons and/or the trapped holes can be released and recombine with each other and luminesce.

2.1.3 Trap Depth

The energy level of the trapped electron is located in the energy gap between the valence band and conduction band of the ideal crystal. The trap depth, E_t, is referred to as the energy gap between the lower edge of conduction band and the energy level of the trap.

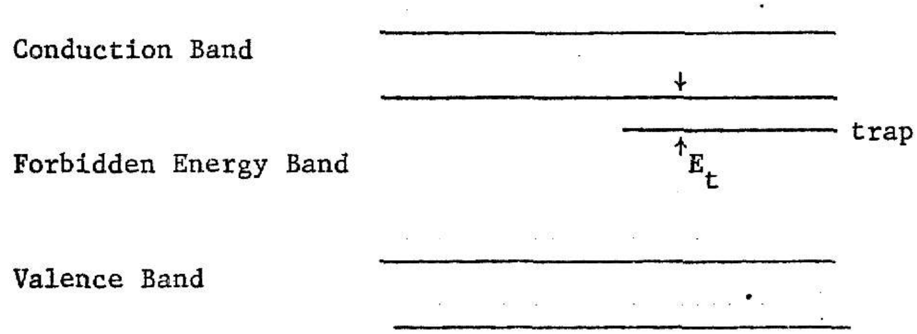

Fig. 1. Energy band of a crystal

2.1.4 Glow Curve

A plot of the luminescence intensity, at constant rate of temperature rise, versus the temperature of an irradiated phosphor is known as the glow curve. The total area under the glow curve is the total light emitted, which is proportional to the absorbed dose. A typical glow curve for CaF_2:Mn (5) is shown in Fig. 2.

THIS BOOK CONTAINS NUMEROUS PAGES WITH DIAGRAMS THAT ARE CROOKED COMPARED TO THE REST OF THE INFORMATION ON THE PAGE.

THIS IS AS RECEIVED FROM CUSTOMER.

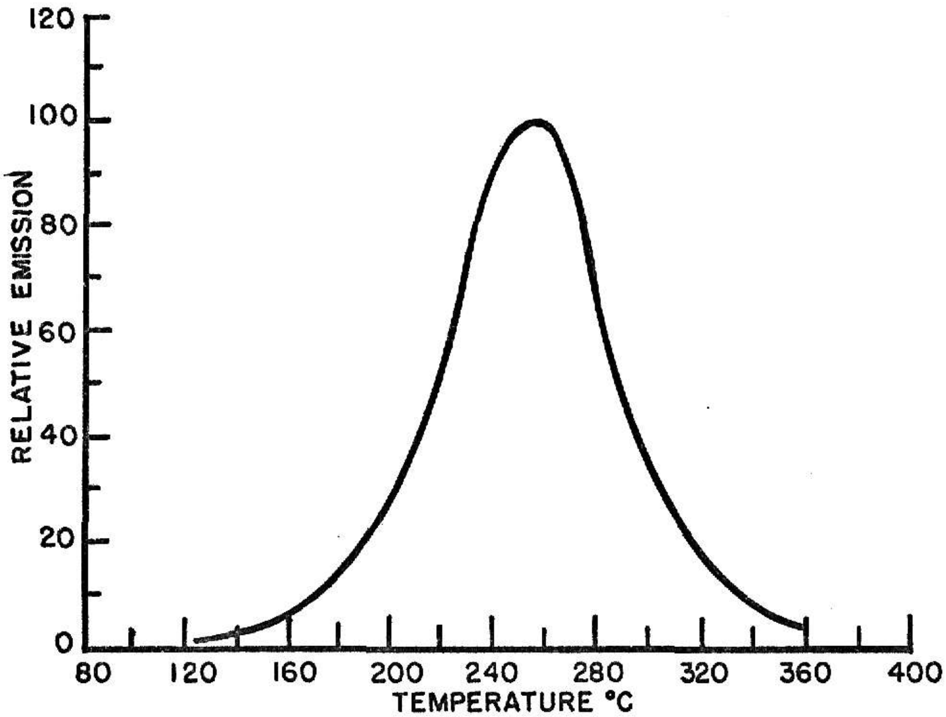

FIG. 2. A TYPICAL GLOW CURVE FOR CaF_2 : Mn

2.2 Several Models of Supralinearity

2.2.1 Model Developed by Cammon, Zimmerman and Bland (6)

This was the first mathematical model developed to explain the TL vs. Roentgens in LiF. It assumes that there are new traps created upon irradiation. The properties of those radiation produced traps are taken to be identical with those originally in the material. If one assumes the proper values for the initial number of unfilled traps, the maximum number of traps and the proportionality constants of trap creation and trap filling, then the model produces a good fit to the experimental data for several measurements on LiF. This model includes an explanation of supralinearity.

2.2.2 Model Developed by Cammon, Suntharalingam and Wilson (7)

In this model, the presence of a competing trap with a cross-section for capturing an electron larger than the dosimetry trap has been assumed. The model also assumes the total number of these competing traps is smaller than the number of dosimetry traps. The competing trap has a larger probability of capturing an electron because of its larger cross-section. As the dose is increased most of the competing traps are filled, and more of the electrons are available in the dosimetry traps. This results in the supralinearity of the response to the radiation dose.

2.2.3 Model Developed by Bloch (8)

After examining the assumption that was made for most of the models that the spectral output of the TL material is the same at low and high absorbed dose, Bloch was led to suspect that the small spectral change during TL could be important since the quantum efficiency of the PM cathode strongly depends on the wavelength of light. To test this possibility, the optical spectrum from the LiF dosimeters was split using a dichoric filter, which transmitted wavelengths longer than 450 nm and reflects shorter wavelengths. Two PM tubes were set to measure the split thermal luminescences. After comparing the results, Bloch concluded that the supralinearity was partially associated with the spectral changes of the TL emission from LiF dosimeters.

2.2.4 Model Developed by Claffy, Klick and Attix (9)

It is proposed that in the case of x-ray and γ-ray irradiations, ionization is produced along the track of an energetic electron and the luminescent centers are close to this track. At low doses, each track is well separated from each other and the TL response arises from the recombinations of holes with luminescent centers occurring in the same track. As the dose increases the tracks begin to interact, so that a hole released from one track during heating may interact with luminescent centers in other nearby tracks, as well as with those in its own track. Thus, an increase in recombination probability results in the observed supralinearity response.

Based upon this model, Dobson and Midkiff (10) derived a dose-TL formula. The formula shows a good fit to some sample data which in turn supports this model.

2.3 Effect of Neutrons

In the ^{252}Cf source fast neutrons are dominant. The mechanism of transferring energy from a fast neutron is to create charged particles by scattering with the TL material. The charged particles produce ionization as they travel through the TLD. Therefore, the models that have been developed for gamma irradiation can apply to neutron irradiation. Thus, a supralinearity is expected in the neutron response of TLD.

3. THERMOLUMINESCENCE DOSIMETRY

3.1 Use of a Phosphor as a Dosimeter

The thermoluminescence technique involves the detection and measurement of the TL output of an irradiated phosphor at an elevated temperature. The TL output is proportional to the number of trapped electrons in the phosphor, which in turn is proportional to the radiation dose the phosphor received. In order to perform as an accurate dosimetric tool, some desirable characteristics of TLD's listed in ref. (5) are:

1) a high concentration of electron and hole traps,
2) high efficiency of luminescence when electrons and holes are thermally released and recombine with each other,
3) long storage of trapped electrons and holes at normal working temperature,
4) a simple trap distribution for greatest simplicity of operation and reading interpretation,
5) a luminescence spectrum which matches the detector and is separated as far as possible from the emission of the heating source,
6) stability of phosphor to radiation.

Spurny (11) also specifies the following desirable properties:

1) no excitation of phosphor other than by radiation,
2) linear response to dose,
3) cheap and reproducible production of phosphor material.

3.2 Factors Affecting the Dosimeter Response

In the following sections, some of the factors that critically affect the response together with reasons for selecting particular methods in this research are discussed.

3.2.1. Preirradiation Annealing

The traps in the TLD's cannot all be depopulated by the heating cycle of the TL reader, so there is a necessity for preirradiation annealing to assure that there are no occupied traps in the dosimeter before using. However, the method of thermal annealing affects the response of TL dosimeter (12). Therefore, it is important to decide upon and adhere to a suitable annealing procedure for consistant results.

For the EG and G TL-39 TLD's used in this research, EG and G has recommended that the dosimeters should be annealed for 5 hours at 350° C if the exposed dose was of the order of 50,000 rad, or until the response of the dosimeters is less than 0.0005 reader unit (13). This annealing procedure has been used by Alexander (14) and Smarsh (15) in their research on CaF_2:Mn and found suitable. Thus it also was adopted in this research.

3.2.2. Postirradiation Annealing

To function as a satisfactory dosimeter, a phosphor should have a TL response that is independent of the storage time at room temperature between the irradiation and reading. Phosphors containing shallow traps produce responses which fade faster than those containing deep traps, and hence are not suitable for dosimetric purposes. Phosphors containing both shallow and deep traps present some potential problems connected with fading. Effects of fading that may be expected in such phosphors are:

1) a reduction in total light output due to the escape of electrons from shallow traps,

2) an increase in the light of the high temperature peaks due to some of these escaping electrons falling into deeper traps.

Since the peak height of the glow curve is taken as a measure of the response in this study, the first effect can be avoided. The details will be discussed in Section 3.2.5. To eliminate the second effect of fading, a post irradiation annealing is used.

For the EG and G TL-31 CaF_2:Mn dosimeters, Alexander (14) found that a partial annealing of the irradiated dosimeters for 7 minutes at 161° C removes the low temperature peak and reduces the spread of the response data. With regard to fading, he found that no significant changes were observed in the TL after partial annealing and storing up to 100 hours. Smarsh (15) used the same procedure to do his research on CaF_2:Mn TL-39 dosimeters and reported satisfactory results. Therefore, this kind of partial annealing was adopted in this research. A typical chart record of the EG and G Model TL-39 dosimeter after partial annealing is shown in Fig. 3.

3.2.3 Types of Radiation

Different types of radiation can affect the response of the dosimeter. These data are not available for CaF_2:Mn dosimeters, but we can see the effects on LiF dosimeters. Morehead and Daniels (16) compared the energy required to procedure an F-center in LiF by different radiations. Their results are presented in Table I.

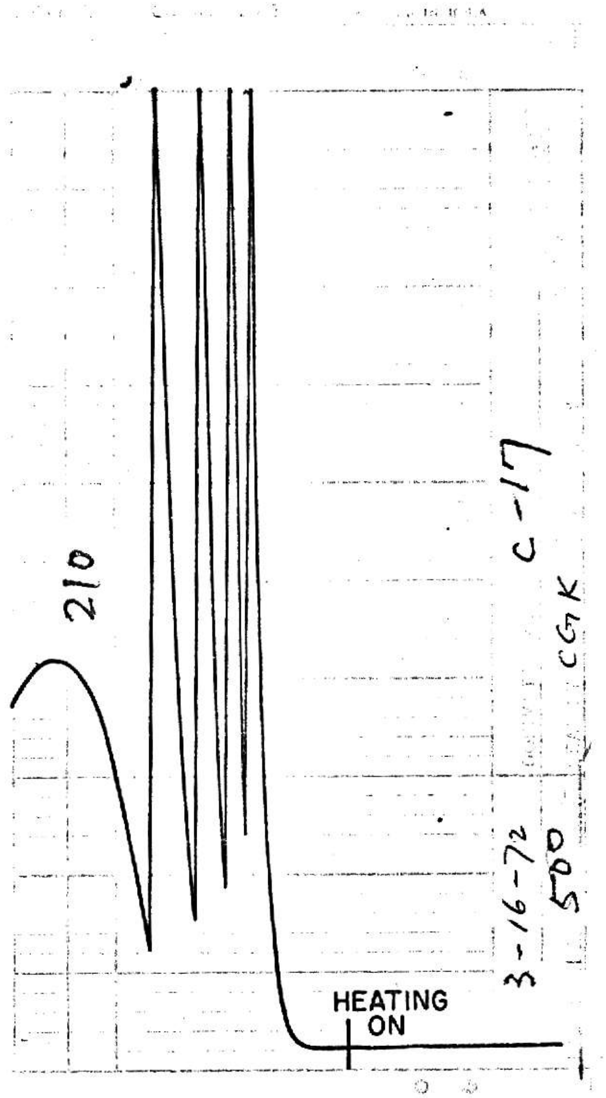

FIG. 3. A TYPICAL CHART RECORD OF THE EG AND G MODEL TL-39 DOSIMETER AFTER PARTIAL ANNEALING.

Table I. Energy (eV) required to produce an F-Center in LiF. (16)

Radiation	Initial	After 10^6 rad	After 10^8 rad
2 MeV alpha particles	700	700	700
2 MeV electrons	140	140	700
1 MeV Gamma Photons	62	160	700
Thermal Neutrons	65	100	700

The different types of irradiation produce different concentrations of F-centers and also effect the glow curve area. Morehead and Daniels (16) determined the glow curve areas under the conditions of different types of radiation and same F-center concentration. The results are presented in Table II.

3.2.4 Physical Characteristics of the Phosphor

The physical characteristics of the dosimeter can affect the response. For example, a larger amount of phosphor can store more energy and emit more light. There is a problem with large samples; the light emitted from the lower layer of the dosimeter can be scattered so that it is not collected by the PM tube. So, due to the variations in the weight, grain size, geometry and other physical characteristics of dosimeters, the responses of individual dosimeter will vary. EG and G company selects its dosimeters so that the variation of response is within $\pm$ 10% in a particular batch of dosimeters.

3.2.5 Quantity Taken to Represent Response

The TL output, which in principle is the area of the glow curve, is proportional to the number of trapped electrons which in turn is proportional to the absorbed dose. However, there are two problems associated with the determination of the area under the glow curve. First of all, the heating elements can emit infrared light which is unwanted in the TL output. Secondly, at low dose the main radiation induced peak ($\sim$ 280°C) is quickly followed by a non-radiation induced tribothermoluminescent peak ($\sim$ 350°C) which is induced in loose powder by mechanical handling (17). In order to solve these problems, it has been found that the height of glow curve is

Table II. Glow curve area produced from F-Center concentration of 2×10^{18} cm^{-3}. (16)

Radiation producing 2×10^{18} F-Center cm^{-3}	Area (in^2/mg LiF)
10^6 rad thermal neutrons	2500
10^6 rad betatrons	2200
1.5×10^6 rad gamma photons	2000
10^7 alpha particles	4000

proportional to the induced TL response if the rate of temperature rise is constant. In addition to the advantages mentioned, the height of glow curve remains the same even though there is a reduction in total light output due to the escape of electrons from shallow traps.

3.2.6 Heating Rate

The glow curve shape is highly dependent upon the heating rate. The peaks in the glow curve appear at higher temperature as the heating rate is increased (1). The magnitudes of the peaks in the glow curve decrease when the heating rate is greater than 30°C/min. (1). For dosimetric purposes, reproducibility of the heating cycle is the most important factor in order to get consistent results.

4. DESCRIPTION OF EQUIPMENT

4.1 Dosimeters

EG and G Model TL-39 "CaF_2:Mn Micro Thermoluminescent Dosimeters" (see Fig. 4) were used in this work. The dosimeters contain 0.8 mg of CaF_2:Mn phosphor in a glass capillary tube 0.9 mm in diameter and 6.0 mm in length, EG and G batch number 10-4-68.

The dosimeters are useful in the dose range from 1 R to 10^5 R (13). The TL response of the dosimeters was linear with respect to dose within $\pm$ 3% (13).

Reproducibility of the dosimeters was reported to be within $\pm$ 3% (13). Due to small fluctuation in phosphor weight, grain size and geometry of sample, the responses of dosimeters in a particular batch were within $\pm$ 10% of the mean (13).

4.2 Reader Unit

An EG and G Model TL-3B Thermoluminescent Dosimeter Reader (Fig. 5) was used to read the dosimeters. The function of the reader unit was to position the dosimeters for readout, provide a reproducible constant heating rate, direct the light emitted toward a photomultiplier (PM) tube and provide a recorder trace of the glow curve.

A block diagram of the recorder unit circuitry is shown in Fig. 6. A regulated current supply of 6.5 ampers fed the read head adapter (described later) in which the dosimeters were positioned. Light emitted by the dosimeters was reflected toward the PM tube. The output signal of the PM tube was fed to a pen-servomechanism through an automatic ranging circuit in the reader unit. The sensitivity of the reader unit was originally set

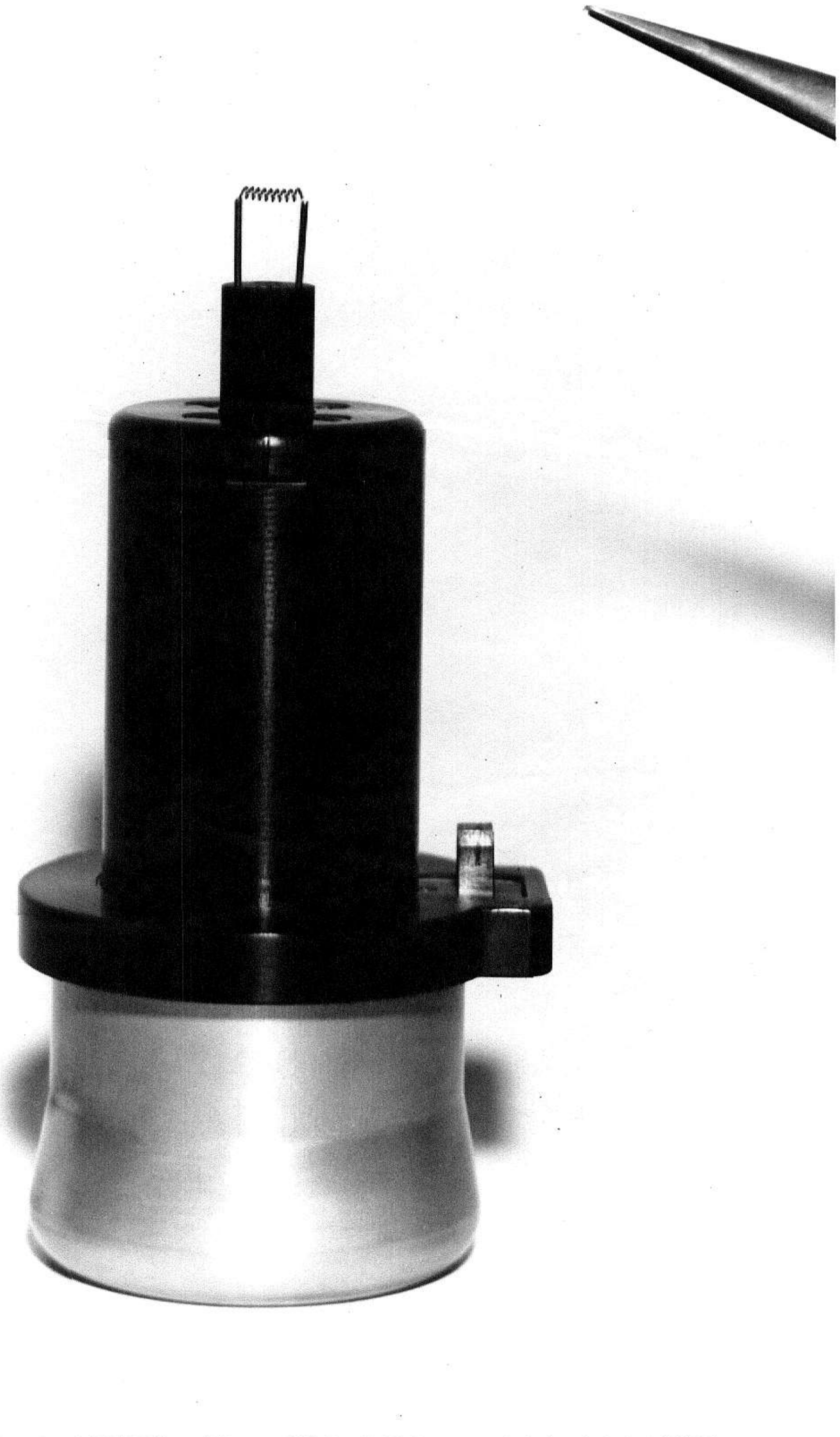

FIG. 4. EG AND G MODEL TL—81A READ HEAD ADAPTER AND TL—39 DOSIMETER.

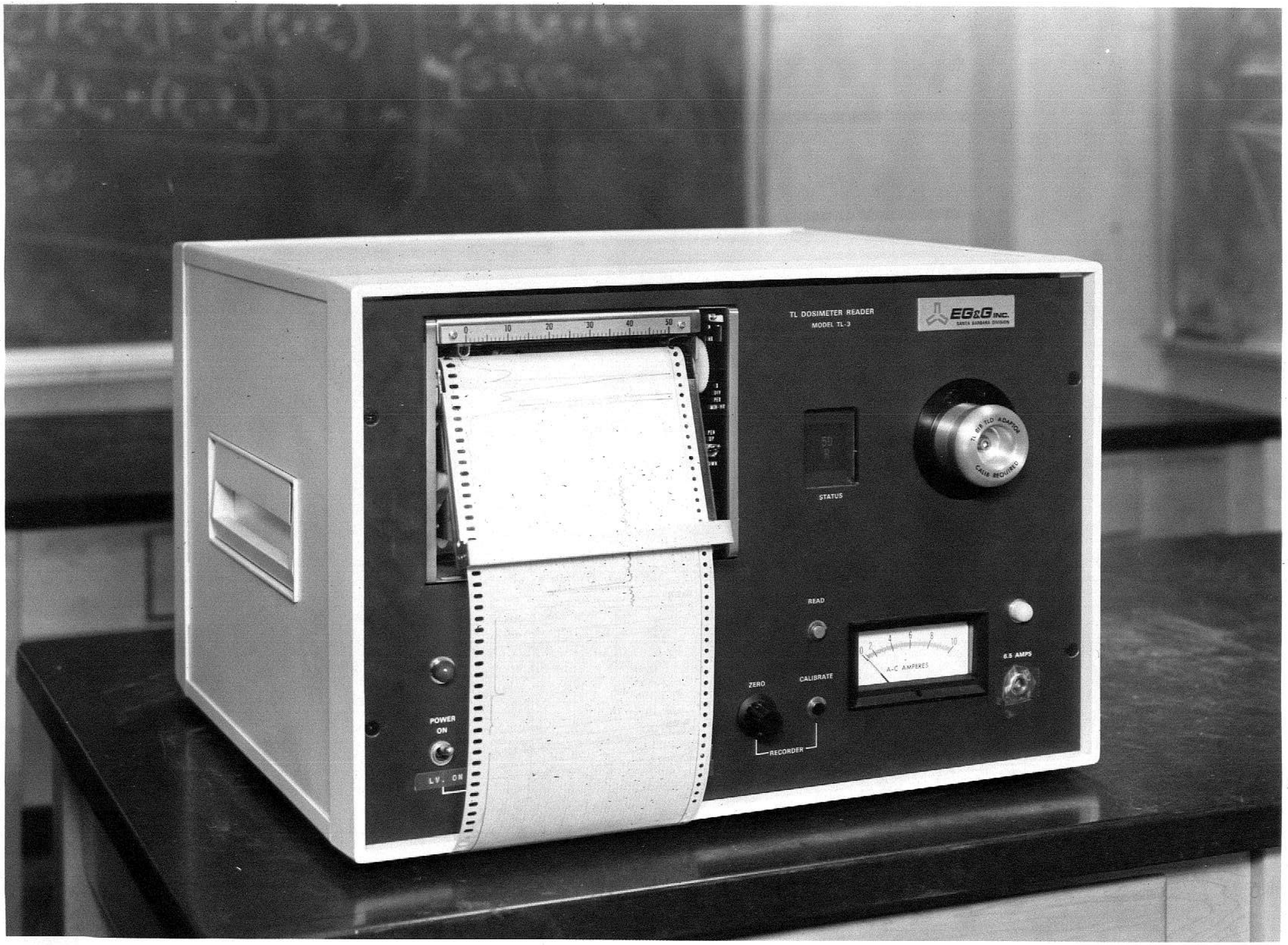

FIG. 5. A VIEW OF THE EG AND G MODEL TL—3B THERMOLUMINESCENT DOSIMETER READER.

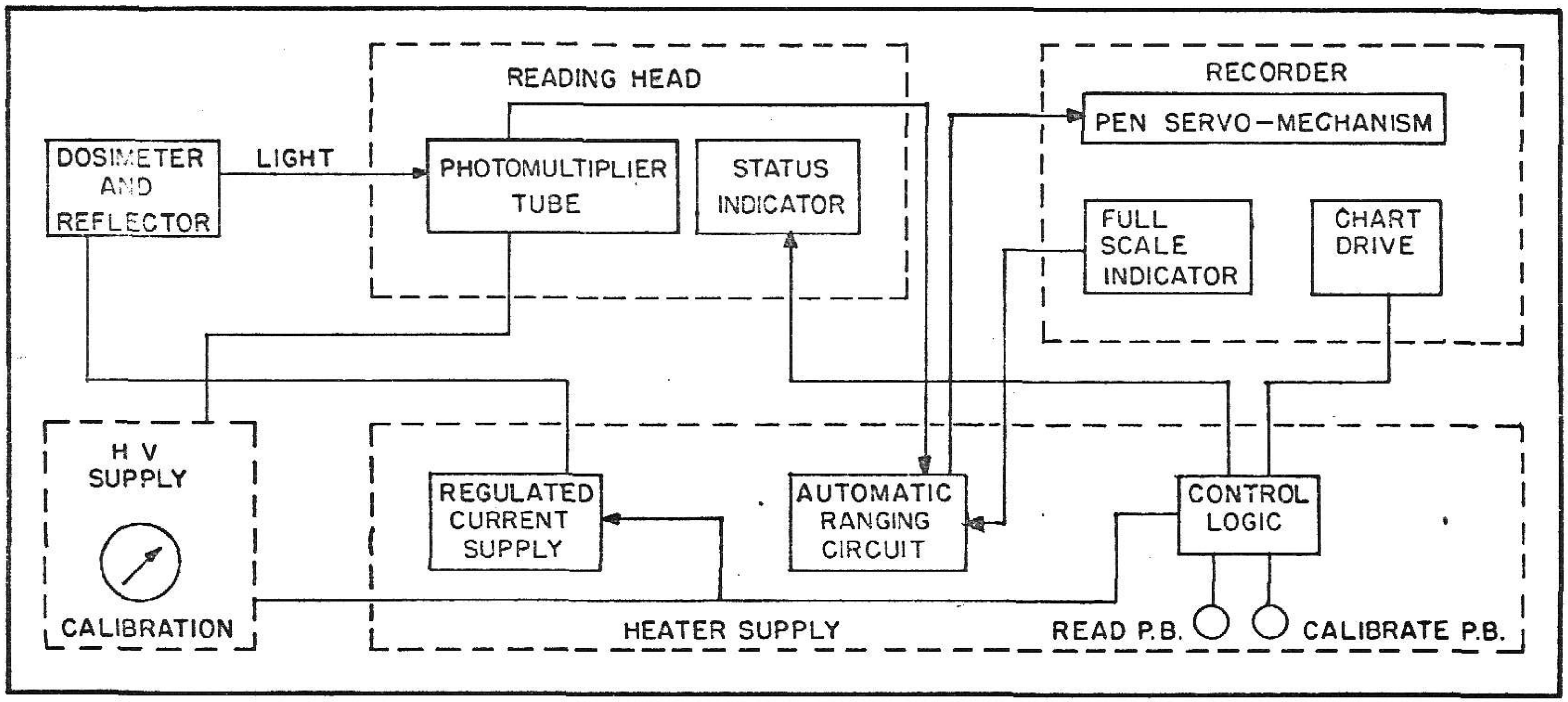

FIG. 6 A BLOCK DIAGRAM OF THE EG AND G MODEL TL-3B READER

to its maximum, which gave the lowest response range of the recorder. When the light output exceeds this range, the automatic circuit lowered the reader sensitivity by a factor of 10. Due to the automatic ranging circuit, the range from 0.050 reader units to 5,000 reader units was covered. After readout of the dosimeter, the status indicator gave the full range of the recorder.

The recorder unit had to be calibrated prior to use. A standard reference dosimeter known as Model TL-32, which was a ^{14}C source intimately mixed with thermoluminescent calcium fluoride, gave a readout of 0.34 reader units. The head adapter used for this reference dosimeter was Model TL-81. The calibration was accomplished by changing the voltage across the PM tube. The normal useful range of the reader was 0.050 to 5,000 reader units. By increasing or decreasing the gain of the PM tube, the range can be extended down to 0.005 reader units or up to 50,000 reader units, at the expense of accuracy.

A typical trace of the glow curve from a TL-39 dosimeters is shown in Fig. 3. The heater current was turned on when the recorder senses the short vertical line near the middle of the chart and turned off at the end of the program (see Fig. 3). An event marker pen produced a vertical "pip" at the top of the chart each time the range changed. Thus the final response range can be determined by counting the number of "pips", or by reading the status indicator.

The EG and G Model TL-81A reader head adapter shown in Fig. 4 was used to hold and heat the Model TL-39 dosimeters in the reader unit. It consisted of a heating coil and a shunt resistance. The regulated current supply provided a constant current of 6.5 amperes through the heating coil. The shunt resistance could be adjusted so that the correct amount of current flowed through the heating coil. This adjustment causes the glow peak to be recorded near the middle of the three lines on the left side of the chart (see Fig. 3).

The final peak height with reference to the final response range shown on the status indicator gave the measure of the thermoluminescence.

4.3 Gammacell

The gamma irradiations were performed with a Gammacell-220 manufactured by the Atomic Energy of Canada, Ltd. The Gammacell was loaded with a 3,963 Ci ^{60}Co source on March 15, 1965. The source was in the form of a hollow cylinder, with twelve linear source elements equally spaced in a stainless steel rack, located inside a thick water shield. The linear element consisted of a welded stainless steel pencil filled with metallic cobalt.

A motor driven plunger, located centrally in a surrounding radiation shield, was driven vertically through the center of the sources. An irradiation chamber, 6-inch in diameter and 8-inch in height, was located in the plunger. The plunger was controlled by a panel beside the unit. The control panel lowered and raised the plunger. The time period of irradiation could be pre-set in the panel and the plunger would automatically raise at the end of the pre-set time. A view of Gammacell is shown in Fig. 7. The dose rate at the time of irradiation was obtained by applying the radioactive-decay formula for ^{60}Co to the results of Kaiseruddin (18).

FIG. 7. A VIEW OF THE GAMMACELL—220 WITH DOSIMETER HOLDER IN PLACE.

4.4 ^{252}Cf facility

Neutron irradiations were performed by a ^{252}Cf source supplied from Savannah River Laboratory. The ^{252}Cf source was in the form of four SR-CF-100 series capsules. Fig. 8 shows the positions of these capsules. The source was loaded on April 1971 and was located on the bottom of a thick water shield. A central thimble, 1.65-inch in diameter, was located in the middle of the source. The samples were put in a dosimeter holder which was inserted into a plastic vial. The plastic vial was lowered to the middle of the source through the central thimble by a string and a pulley. The overall view, and the cross-section view of the ^{252}Cf facility are shown in Fig. 9 and Fig. 10 respectively. ^{252}Cf has an effective half-life of 2.646 years and continuously emits neutrons with a fission spectrum.

After each irradiation, two tests were made to be sure that the sample capsule was safe enough to handle. If the activity, as measured by a G-M tube, was less than 5 mR/hr, the sample capsule could be handled. If the activity were greater than 5 mR/hr, the sample capsure could not be opened until the activity was less than 5 mR/hr. The second test was for surface contaminants. The surface of the sample capsule was wiped with filter paper until the activity on the filter paper was less than 100 counts per second as measured by a G-M counter and an associated Nuclear Chicago Model 1619A rate meter.

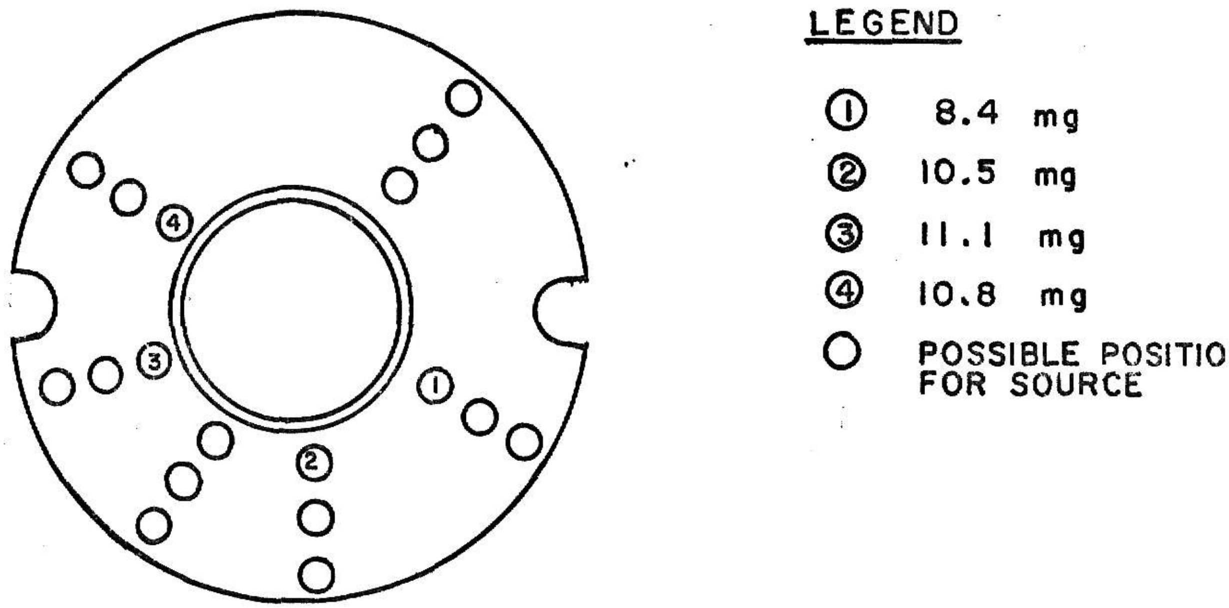

FIG. 8. PLEXIGLASS ^{252}Cf SOURCE HOLDER WITH SOURCE LOCATIONS.

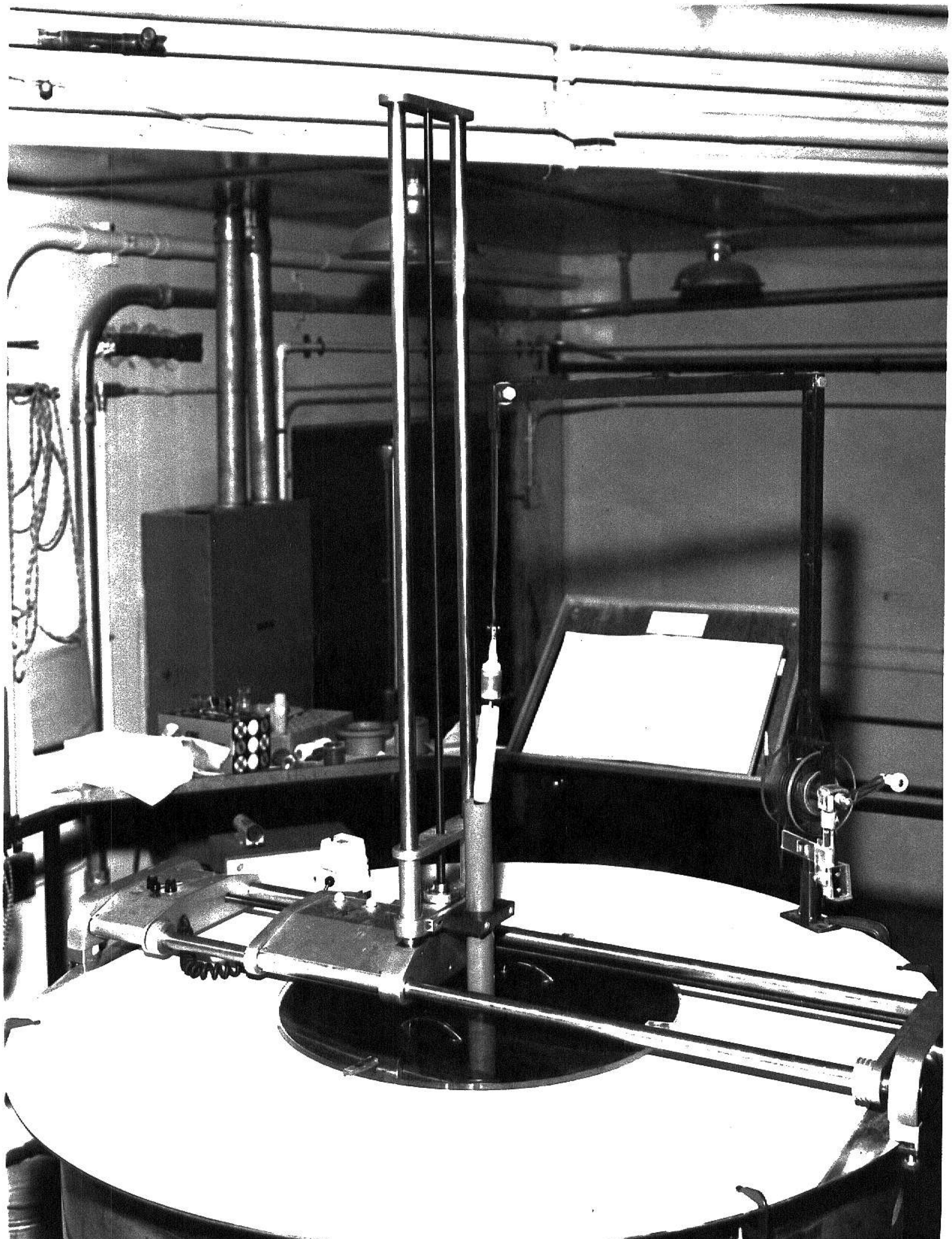

FIG. 9. A VIEW OF THE ^{252}Cf FACILITY AT K.S.U.

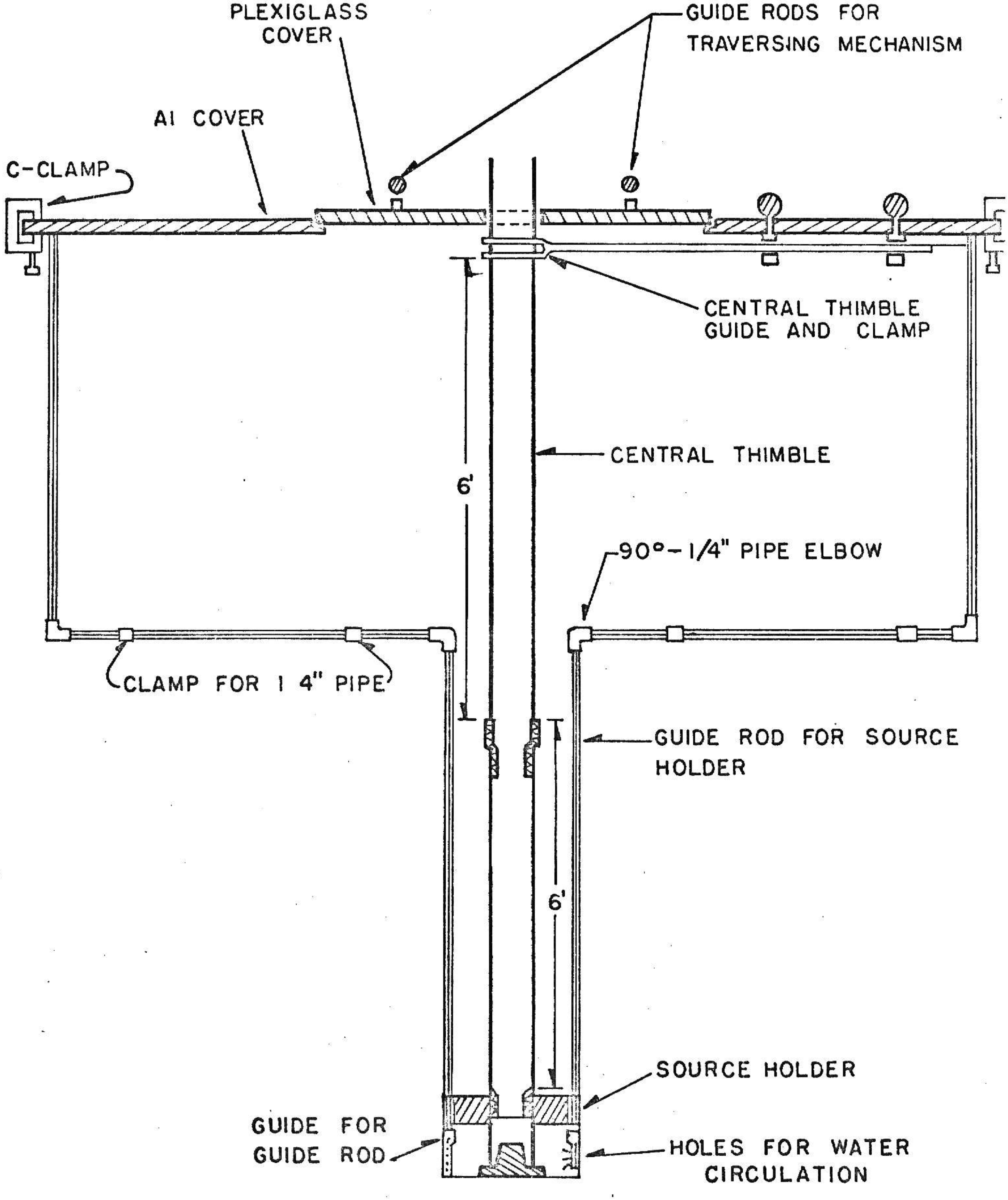

FIG. 10. A CROSS SECTION VIEW OF THE
^{252}Cf FACILITY.

5. DETERMINATION OF GAMMA-RADIATION CALIBRATION CURVE

5.1 Necessity

It is a standard procedure in thermoluminescence dosimetry to calibrate the dosimeters prior to use (18). In this study, it was also necessary to calibrate the dosimeters since they had been used before, and it was suspected that they might have developed permanent lattice defects which would have changed their characteristics. To make sure that this had not happened, a gamma calibration curve was obtained before the neutron calibration curve. The peak height measured on the glow curve plotted by an EG and G reader gave the response of the dosimeters in reader units. A full calibration curve is required to convert the reader units into radiation units.

5.2 Equipment and Technique

In order that all dosimeters receive the same dose at each experimental point, a satisfactory dosimeter holder was needed. According to the specifications by manufacturer, the isodose curve was 2.75-inches above the base of the irradiation chamber and 2-inches from the vertical axis. The dose received on the isodose curve was the same as that at the center of the chamber. A 1/2-inch polyethylene disk was made to fit the irradiation chamber. There were 24 positions for dosimeters on the circumference of a 4-inch circle on the disk. Three legs, 2.05-inches in height, were used to support the disk. By placing the dosimeters in the holes of the disk, they received the same dose.

The timer on the gammacell was used to measure the irradiation time. However, the timer started counting when the plunger was at its lowest position, the dosimeters were irradiated as the plunger moved up and down. Since the traverse time was constant, so was the dose. Then the total dose, D, is given as

$$D = D_o + \dot{D}t \tag{5.2-1}$$

where D_o is the constant dose due to traverse time

$\dot{D}$ is the dose rate

t is the irradiation time.

Over the linear portion of the calibration curve, the total response R, of the dosimeters in reader units is given as

$$R = R_o + \dot{R}t \tag{5.2-2}$$

where R_o is the constant response due to the dose received in the traverse time

$\dot{R}$ is the dose rate in reader units.

The parameters of R_o and R can be obtained by a weighted least square analysis on the experimental data. $\dot{D}$, the dose rate, was a known value at the time of irradiation. The calibration factor, K, with units of rads per unit reader unit could be determined as the division of $\dot{D}$ by $\dot{R}$. The values of D_o thus could be obtained by the multiplication of R_o and K.

5.3 Experimental Procedure

To determine the calibration curve, eighteen dosimeters were irradiated at the same time for each experimental point. Before the irradiation, the dosimeters were placed in a graphite block and annealed at 350°C for 5 hours or more.

Following the irradiation, the dosimeters were partially annealed at 161°C for 7 minutes. After removal from the oven, the dosimeters were cooled to room temperature before being read out.

5.4 Analysis of Data and Results

For each experimental point, the mean value and standard deviations were calculated. These values are presented in Appendix A. The first four data points were used in the linear regression for the determination of R_o and $\dot{R}$. The values obtained from the linear regression were R_o = 2.875 reader unit and $\dot{R}$ = 1.0039 reader unit/sec. The calibration factor, K, was obtained by dividing the known dose rate of 35.73* rad/sec by $\dot{R}$. Thus, the value obtained for K was 35.59 rad/reader unit.

The calibration factor times R_o gave the travel dose, D_o, as 102.36 rad. The timed dose was the dose rate multiplied by the irradiation time. The total dose was the sum of travel dose and timed dose. All these values are presented in Appendix A. In Fig. 11, the total dose is plotted as the abscissa and the experimentally determined response as the ordinate to give the full calibration curve.

From the results of previous work (14) (15) (18) (19) we know that there is a linear region and psuedo-linear. Therefore the calibration curve was divided into three dose ranges; the low dose range (0 to 9,749 rad), the intermediate dose rage (10,821 to 85,854 rad) and the saturation dose range (above 128,730 rad). The curve shown in Fig. 11 was obtained as follows. In

---

* $\dot{D} = \dot{D}_o \exp\left(-\frac{0.6931 \times t}{t_{1/2}}\right)$, $\dot{D}_o = 3.27 \times 10^5$ rad/hr

$t_{1/2}$ = 62.4 months, t = 82 months.

the low and intermediate dose ranges the data were fitted to a linear model in each range using a weighted least square analysis. The results are presented in Table III. The linear equations obtained for the low dose range was $R = 0.0273\ D + 0.1530$ and for the intermediate dose range was $R = 0.0353\ D - 97.658$. The two lines shown in Fig. 11 are plots of the above equations. The supralinearity is not shown clearly on the logarithmic scales; however, the equations show the ratio of the slope in the intermediate dose range to that in the low dose range is 1.293. The break point of these two regions is between 9749 rad and 10821 rad (corresponding to 253 R.U. and 279 R.U.). Evidence of saturation began at about 10^5 rad. These results are in agreement with the results of Smarsh (15).

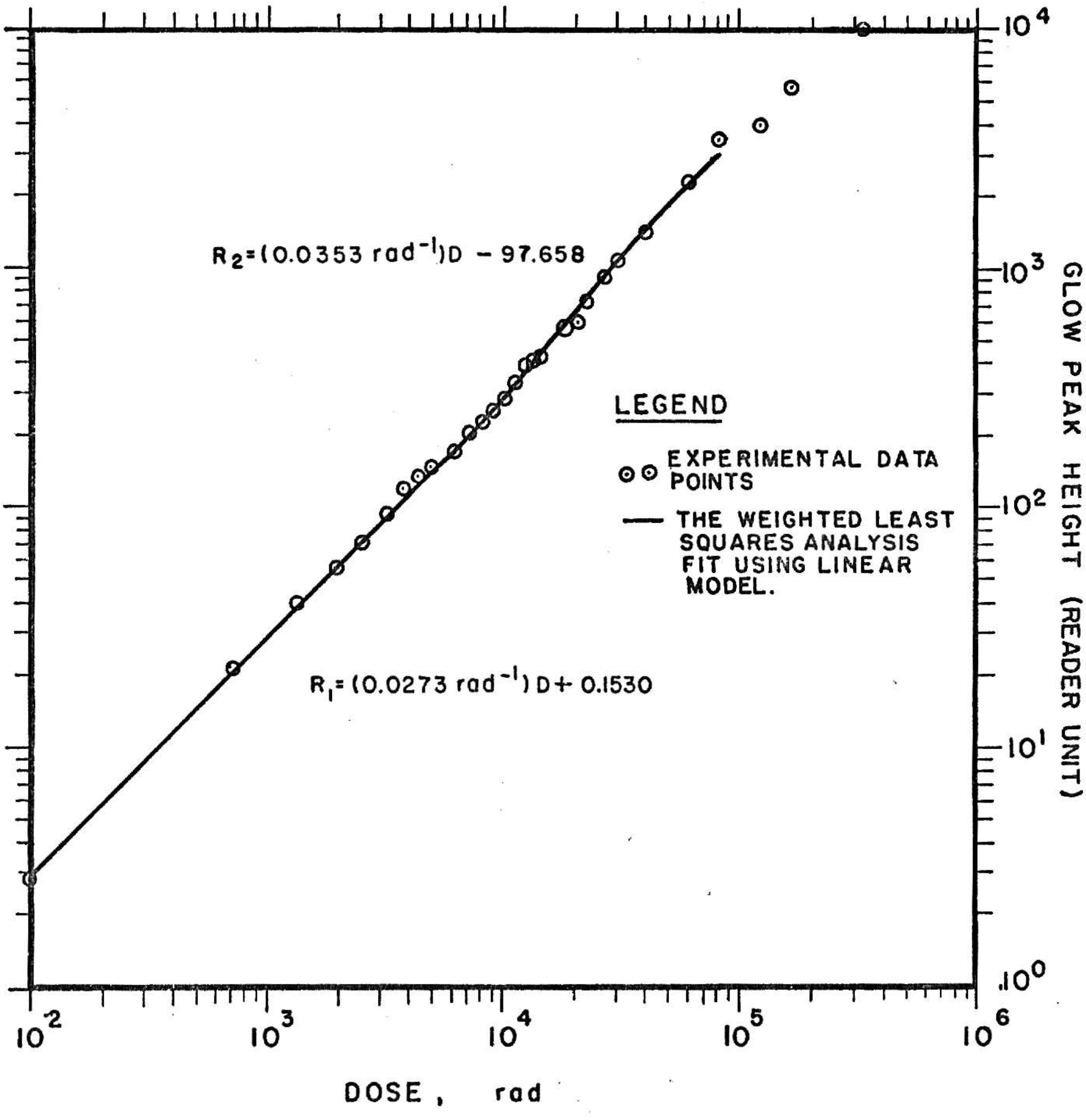

FIG. 11. THE GAMMA CALIBRATION CURVE FOR EG AND G MODEL TL-39 $CaF_2:Mn$ DOSIMETERS.

Table III. Values of Parameters Derived from the Gamma Calibration Curve by a Weighted Least Squares Analysis

	slope (reader unit/rad)	y-Intercept (reader unit)
Low Dose Region	0.0273 ± 0.0123	0.1530 ± 0.0824
Intermediate Dose Region	0.0353 ± 0.0288	-97.658 ± 48.1629

6. THE ESTIMATION OF FAST-NEUTRON FLUENCE FROM THE ^{252}Cf SOURCE

6.1 Necessity

The peak height from the glow curve was in relative units. A neutron calibration curve was required to convert the relative units into fast neutron fluence. Estimation of fast neutron fluence was done semi-experimentally before the calibration curve was determined.

6.2 Equipment and Technique

Since the half-life of the ^{252}Cf was quite long compared to the irradiation time, the flux was assumed to be constant. The fluence thus was the product of flux and irradiation time.

With the ^{252}Cf capsules in the configuration, as shown in Fig. 8, a fast neutron spectrum was obtained with 1/2" NE-213 proton recoil detector at the distance of 2'9" from the ^{252}Cf capsules (position A) by Prigel (20). This fast neutron spectrum is reproduced as Fig. 12 with the magnitude enlarged by a factor of 4.5×10^3. By integrating graphically the area under this spectrum, the fast neutron flux at position A was found to be 218.25 n/cm^{2}sec.

In order to normalize the 1/2" NE-213 proton-recoil detector, Prigel (20) unfolded a PuBe spectrum from 2" NE-213 proton recoil detector, which is an absolute detector, and from 1/2" NE-213 proton-recoil detector. Comparing these two results, the ratio of the absolute fast neutron flux to the fast neutron flux obtained from 1/2" detector was 4.5×10^3. Therefore, the absolute fast neutron flux at position A was (218.25 n/cm^{2}sec) x (4.5×10^3), i.e., 9.82×10^5 n/cm^{2}sec.

So far, the absolute fast neutron flux at position A was known. The main interest was to find out the absolute fast neutron flux at the center of the

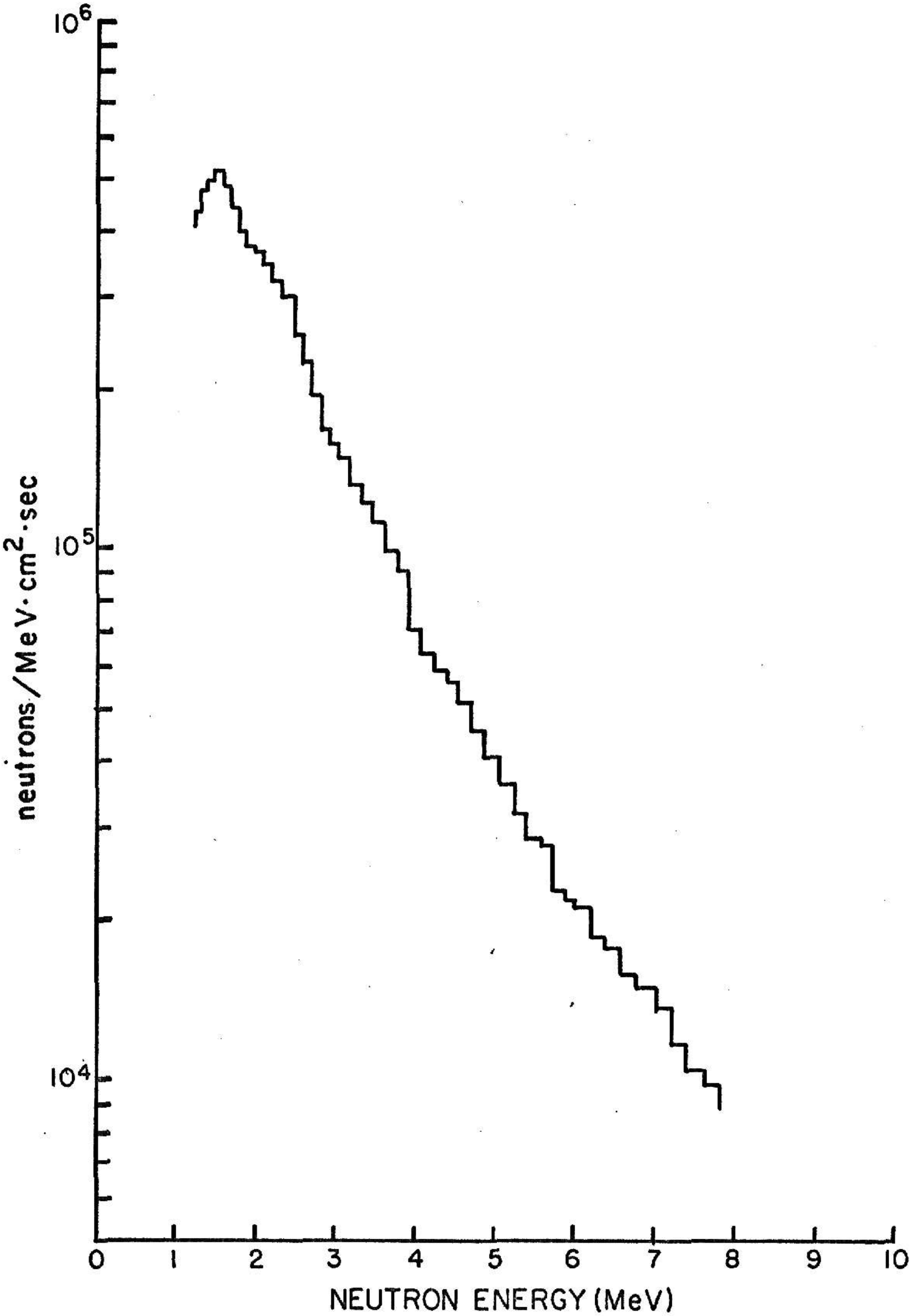

FIG. 12. NEUTRON SPECTRUM WITH 1/2 INCH NE-213 DETECTOR AT POSITION A IN THE ^{252}Cf SOURCE (20).

^{252}Cf capsules (position B). Two methods have been used to relate the fast-neutron fluxes at position A and at position B. One was a nickel foil activation method, the second was an extrapolation of the dose rate versus thickness of water shield from a point source of ^{252}Cf. These two analyses are presented as follows.

6.2.1 Nickel foil activation method

$^{58}Ni(n,p)^{58}Co$, having an effective cross-section of 0.420 barn, was the primary reaction in this analysis. ^{58}Co decayed with a half-life of 71.4 days and emitted a 0.811 MeV gamma ray. Due to the relatively long half-life, this reaction could be used to monitor the fast-neutron flux without considering ^{58}Co decay during the irradiation and with no requirement to count the nickel foil immediately.

The counting system used to measure the ^{58}Co activity in the nickel foils consisted of 3" by 3" cylindrical NaI(Tl) well-type scintillation detector with associated photomultiplier tube, preamplifier and high voltage supply. The gamma ray spectrum of the induced ^{58}Co activity was accumulated in a TMC 100 channel Analyzer. The analyzer gain was set such that the peak of the 0.811 MeV ^{58}Co gamma ray fell in approximately channel 60. For further details of the theory and techniques see Thiesing (21). A typical pulse-height spectrum from an irradiated nickel foil is shown in Fig. 13.

The equation that is used to calculate the fast neutron flux is

$$K\phi = \frac{C(t_i + T)\, e^{\lambda t}}{M_n\, t_c\, t_i} \qquad (6.2.1\text{-}1)$$

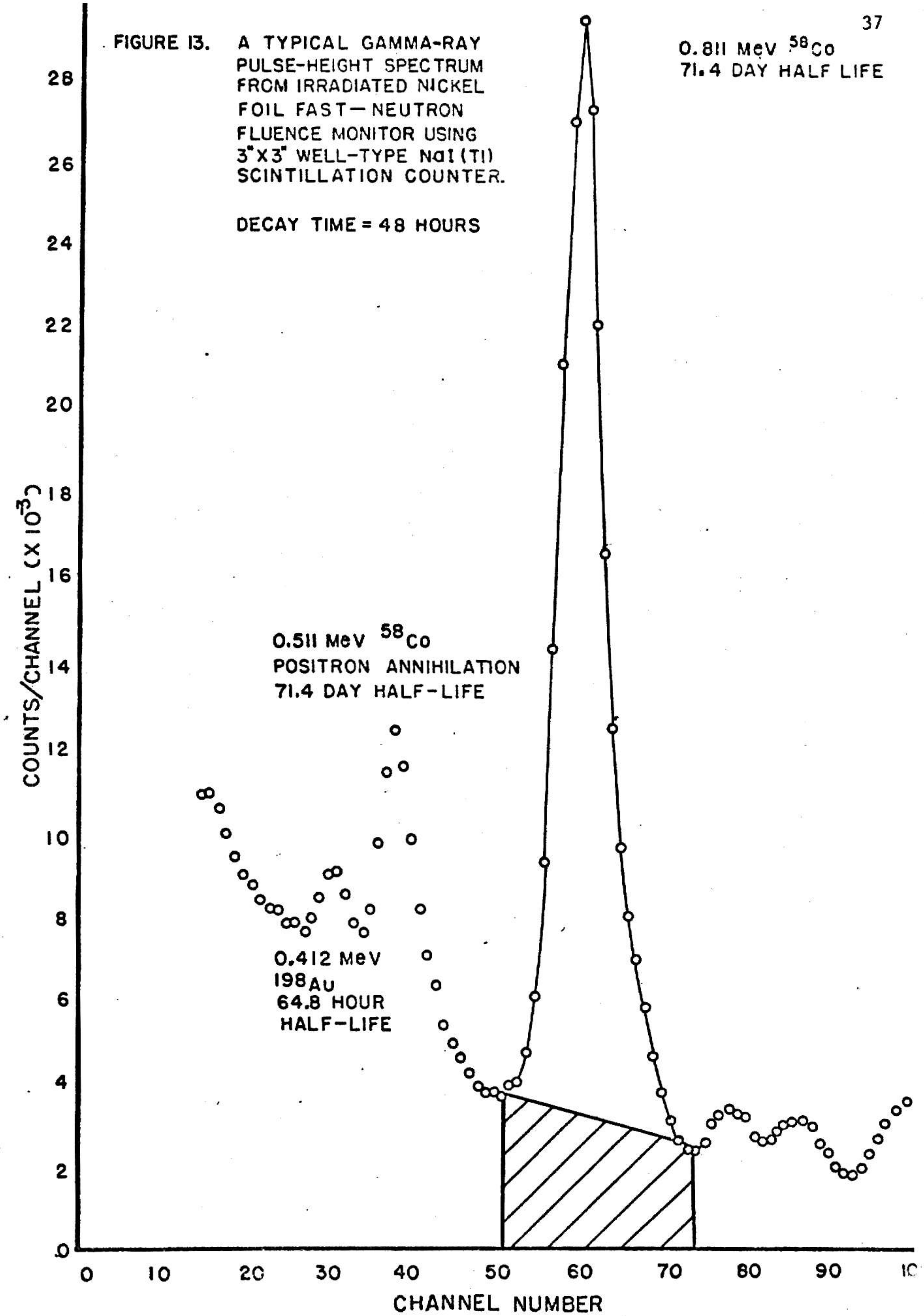
FIGURE 13. A TYPICAL GAMMA-RAY PULSE-HEIGHT SPECTRUM FROM IRRADIATED NICKEL FOIL FAST—NEUTRON FLUENCE MONITOR USING 3"X3" WELL-TYPE NaI(Tl) SCINTILLATION COUNTER.
DECAY TIME = 48 HOURS
0.811 MeV 58Co
71.4 DAY HALF LIFE
0.511 MeV 58Co
POSITRON ANNIHILATION
71.4 DAY HALF-LIFE
0.412 MeV
198Au
64.8 HOUR
HALF-LIFE
COUNTS/CHANNEL (X 10-3)
CHANNEL NUMBER
0
10
20
30
40
50
60
70
80
90
.0
2
4
6
8
10
12
14
16
18
20
22
24
26
28

where $K \equiv$ constant for all foils,

$\phi \equiv$ the relative fast neutron flux,

$C(t_i + T) \equiv$ observed counts due to 0.811 MeV gamma rays of ^{58}Co,

$\lambda \equiv$ decay constant of ^{58}Co,

$M_n \equiv$ mass of foils,

$t_c \equiv$ counting time of foils,

$t_i \equiv$ irradiation time of foils,

$T \equiv$ decay time of foils.

Following the procedure and techniques suggested by Thiesing (21), the nickel foil activation analysis have been done on position A and position B in the ^{252}Cf source. The results are presented in Table IV.

From the results in Table IV, the ratio of fast neutron flux at position B to that at position A was $\frac{24.74}{4.04 \times 10^{-3}}$, i.e., 6.12×10^3. The flux at position A was 9.82×10^5 n/cm^2 sec in section 5.2. So the flux at position B was 6.01×10^9 n/cm^{2}sec.

6.2.2 By Chart of Dose Rate vs. Thickness of Water

In reference (22), there is a chart of dose rate at the surface of water shield source of ^{252}Cf. It is shown in Fig. 14. In Fig. 14 the shortest valid distance is about 12 cm. The distance between position B and the center of the source was approximately 3 cm. By extrapolating the curve to the point of thickness 3 cm, the dose rate value (relatively) was 1.2×10^{-1}. The dose rate value (relatively) at position A was 2×10^{-5}. By assuming the dose rate ratio is equal to the fast neutron flux ratio, the fast neutron flux at position B is determined as $(9.82 \times 10^5$ n/cm^{2}sec$) \times (\frac{1.2 \times 10^{-1}}{2 \times 10^{-5}})$, i.e., 5.89×10^9 n/cm^{2}sec.

Table IV. Data and Results of Nickel Foil Activation Analysis

	Position A	Position B
$C(t_i + T)$	2,668 counts	86,270 counts
t_i	400 min.	40 min.
t_c	915 min.	120 min.
T	58 hours	54.1 hours
Mn	1.823 gm	0.904 gm
$K\phi$	4.04×10^{-3}	24.74

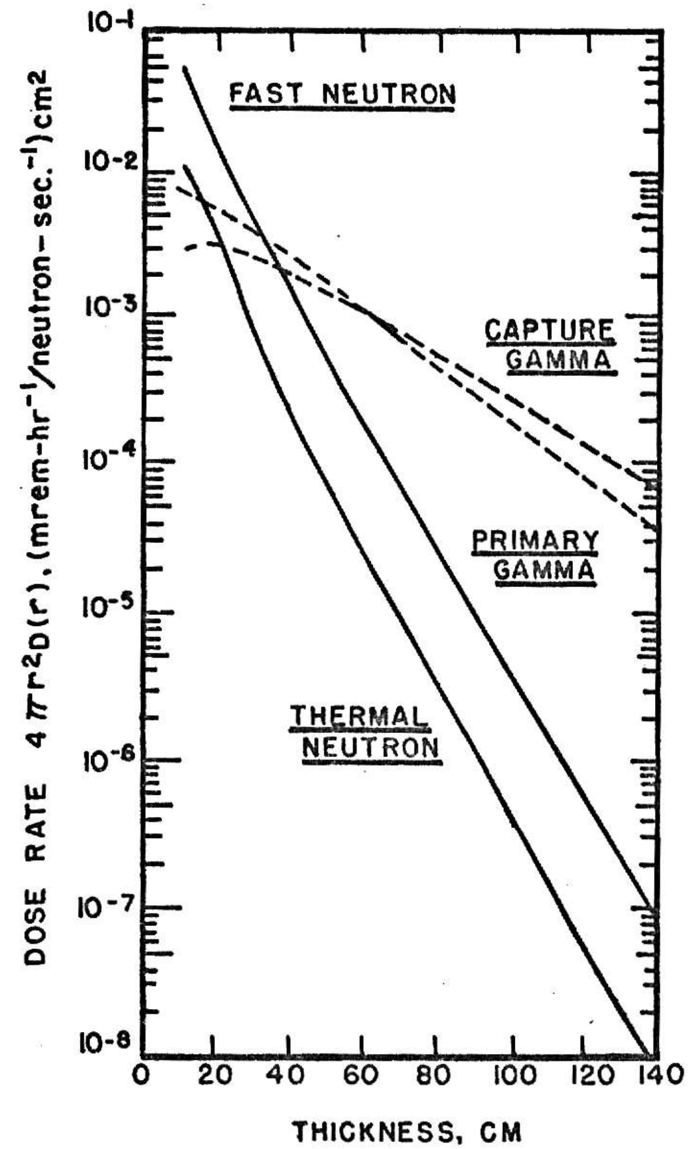

FIG. 14. DOSE RATE AT SURFACE OF WATER SHIELD FROM A POINT ISOTROPIC FISSION SOURCE OF CALIFORNIUM-252 (22).

6.3 Summary

The fast neutron fluxes obtained from two different methods are very close to each other. In this study, the value of 6.0×10^9 n/cm^{2}sec has been accepted as the fast neutron flux at position B, the center of the ^{252}Cf source.

7. DETERMINATION OF NEUTRON CALIBRATION

7.1 General Considerations

The neutron calibration curve was inherently more difficult than the gamma calibration. The dose rate in the gammacell was known, but the dose rate of ^{252}Cf sources was not well determined. A calibration curve was expressed in the relative units of the peak height from the EG and G reader to the fast neutron fluence.

7.2 Equipment and Technique

The ^{252}Cf source was used to irradiate the dosimeters for calibration. The dosimeters were placed on the circumference of a polyethylene holder, 1-inch in diameter and about 2-inch thick. This dosimeter holder fits in the bottom of a polyethylene capsule. The polyethylene capsule was then placed in the central thimble of the ^{252}Cf source. The four ^{252}Cf capsules were in the configuration shown in Fig. 8.

There is no electrical means to move the samples in the ^{252}Cf source as in the ^{60}Co Gammacell. A pulley was used to move the capsule holding the dosimeters. The travel time was about 10 seconds. It was shown experimentally that the dose received by the dosimeters during the period of traveling was far less than 1 reader unit from the TLD reader. Therefore, in this study the effect due to traveling was neglected. The time mentioned here is the period that the capsule was at its lowest position.

Over the linear portion of the calibration curve, the response, R, of the dosimeters in reader units, was given as

$$R = \dot{R}F \tag{7.2-1}$$

where $\dot{R}$ ≡ calibration factor, R.U./(n/cm^2)

F ≡ fluence, n/cm^2

7.3 Experimental Procedure

The dosimeters were first annealed at 350°C for 5 hours or more and then were cooled to the room temperature. After cooling, 18 dosimeters were irradiated for the same time. Fluence was determined by the product of the flux and the irradiation time. Following the irradiation, the dosimeters were partially annealed at 161°C for 7 minutes after they were cooled to room temperature, the dosimeters were ready to read out.

7.4 Analysis of Data and Results

The mean value and the standard deviation were calculated for each experimental point. These values are presented in Appendix B. In Fig. 15, the fluence is plotted as the abscissa and the experimentally determined points as the ordinate for the calibration curve.

Using the same argument stated in gamma calibration curve, the calibration curve was divided into three regions; low fluence region, intermediate fluence and saturation fluence regions. A weighted least square analysis was used to fit a straight line through the low fluence region and another one through the intermediate fluence region. The two lines shown on the calibration curve are the straight lines fitted to least square analysis in two regions respectively. The results of least squares analysis are shown on Table IV.

The slope of the straight line in the intermediate fluence region is 1.305 times the slope of the straight line of low fluence region. The evidence of saturation region is seen at the fluence equal to 1.80×10^{14} n/cm^2.

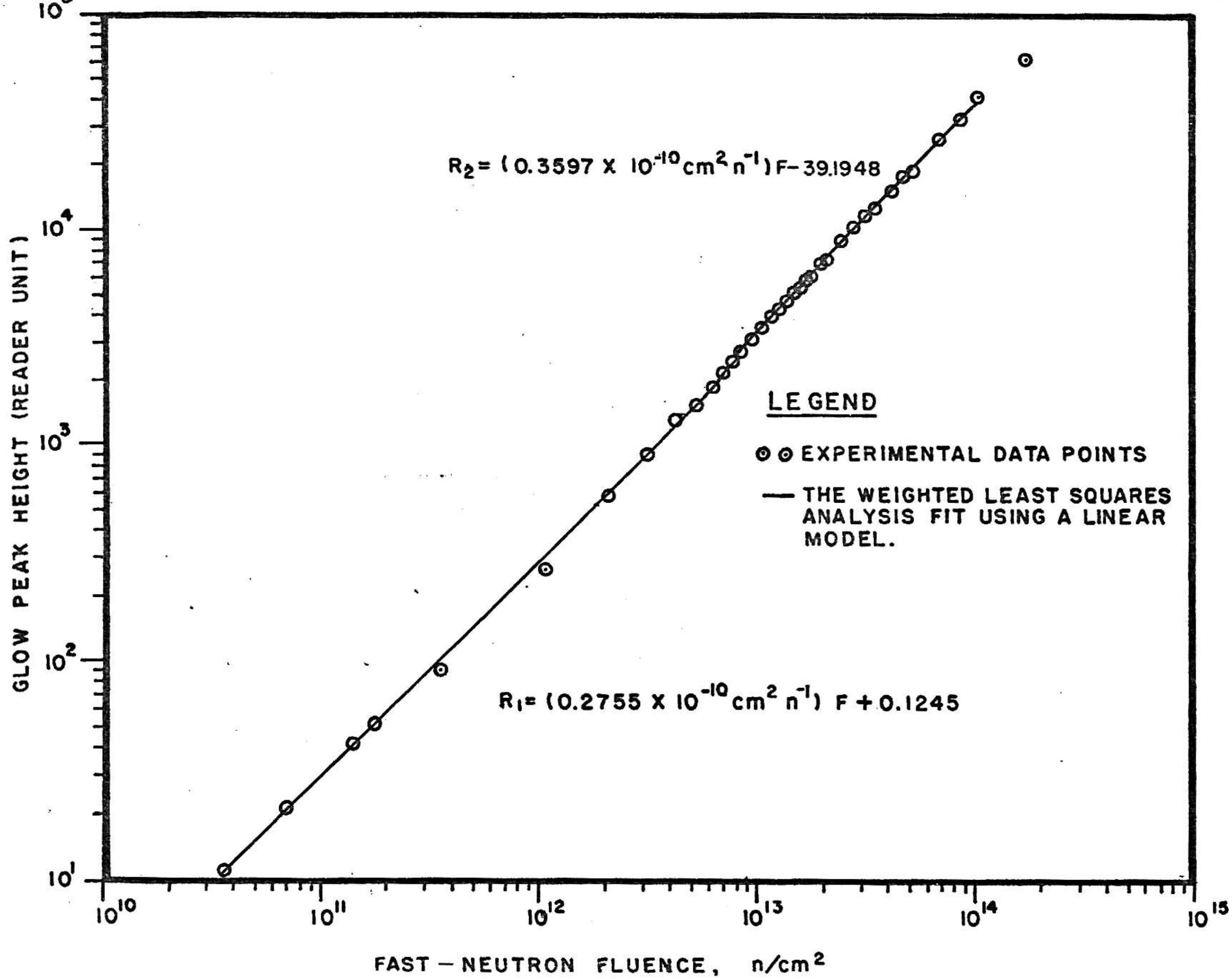

FIG. 15. THE NEUTRON CALIBRATION CURVE FOR EG AND G MODEL TL-39 CaF_2: Mn DOSIMETERS

Table V. Values of Parameters Derived from the Neutron Calibration Data by a Weighted Least Squares Analysis

	slope, (reader unit/(n/cm^2))	y-Intercept, (reader unit)
Low Fluence Region	$(0.2755 \pm 0.0135) \times 10^{-10}$	0.1245 ± 0.0135
Intermediate Fluence Region	$(0.3597 \pm 0.0189) \times 10^{-10}$	-39.1948 ± 31.5180

8. DISCUSSION AND CONCLUSIONS

8.1 Discussion of Results

The supralinearity in the calibration curve has been shown both in gamma calibration curve and neutron calibration curve. This is sufficient to say decisively that the response of EG and G Model TL-39 CaF_2:Mn dosimeters has the property of supralinearity. This can be explained qualitatively by the various models developed for gamma irradiation mentioned in chapter 2. In this study, there was only one kind of CaF_2:Mn dosimeters used. Qualitatively similar results might be expected for other kinds of CaF_2:Mn dosimeters.

Comparison between the gamma calibration curve obtained by Smarsh (16), and the gamma calibration curve and the neutron calibration curve obtained in this research, there are several facts that should be noticed.

1) All calibration curves occur the supralinearity at between the response of 200 R.U. to 300 R.U.
2) The slope of the intermediate dose range is 1.3 times that of the low dose range in all the calibration curves.
3) The evidence of saturation start at approximately 4,000 R.U. in all three calibration curves.

8.2 Conclusions

There were three main conclusions drawn from this study.

1) The response of CaF_2:Mn dosimeters to the neutrons from ^{252}Cf source is not linear; the supralinearity occurs at between the fast-neutron fluence of 7.20×10^{12} and 7.92×10^{12} n/cm^2.

2) The slope of the intermediate fluence range in the calibration curve is 1.305 times the slope in the low fluence range.

3) The saturation range in the neutron calibration curve starts at approximately 1.80×10^{14} n/cm^2.

9. SCOPE FOR FUTURE WORK

There are many areas that need investigating in the field of thermoluminescent dosimetry.

Further work that may be done in the theoretical explanation to the supralinearity in the gamma calibration curve and neutron calibration curve. The models suggested today only give a qualitative explanation. There should be a more sophisticated theory to this phenomenon.

Another area of investigation is the discrimination of radiations in a mixed radiation field by the TL dosimeters. The practical value of TL dosimetry would be enlarged greatly if this can be done.

The effects of the saturation study including the type and extent of any radiation damage is another area for further study. Included in this study could be the effect of dose rate on saturation. Low temperature studies on the CaF_2:Mn dosimeter is another area which may offer clues to the mechanism of TL.

10. ACKNOWLEDGEMENT

The author is indebted to many people who aided in the completion of this work: to Dr. Hermann J. Donnert and Dr. J. F. Merklin for their guidance and encouragement; to Don Prigel and Tom Roberts for their cooperation; and to Mohammed Kaiseruddin for his suggestions and help.

Financial support from the Department of Defense Themis Project, administered through the Office of Naval Research, is gratefully acknowledged. A sincere expression of love and gratitude is extended to the author's wife who because of her encouragement and typing have made this work possible.

11. LITERATURE CITED

1. Cameron, J. R., N. Suntharalingam and G. N. Kenney, Thermoluminescent Dosimetry, The University of Wisconsin Press, 1968.

2. Ginther, R. J. and R. D. Kirk, "The Thermoluminescence of CaF_2:Mn," J. Electrochem. Soc., 104, 365 (1957).

3. Schulman, J. H. et al., "New Thermoluminescent Dosimeter," Rev. Sci. Instr., 31, 1263 (1960).

4. Spinks, J. W. T. and R. J. Woods, "An Introduction to Radiation Chemistry," John Wiley & Sons, Inc., New York (1964).

5. Schulman, J. H., "Survey of Luminescence Dosimetry," Luminescence Dosimetry, ed. F. H. Attix, (U.S. Atomic Energy Commission, Division of Technical Information, Oak Ridge, Tennessee, 1967), 7.

6. Cameron, J. R., D. W. Zimmerman and R. W. Bland, "Thermoluminescence vs. Roentgens in LiF: A Proposed Mathematical Model," Luminescence Dosimetry, ed. F. H. Attix, (U.S. Atomic Energy Commission, Division of Technical Information, Oak Ridge, Tennessee, 1967), 47.

7. Cameron, J. R., N. Suntharalingam and C. R. Wilson, "Supralinearity of Thermoluminescent Phosphors," Proc. of the Second International Conference on Luminescence Dosimetry, ed. J. A. Auxier, et al. (U.S. Atomic Energy Commission, 1968), 332.

8. Bloch, P., "Supralinearity in LiF," Proceedings of the Second International Conference on Luminescence Dosimetry, ed. J. A. Auxier, et al. (U.S. Atomic Energy Commission, 1968), 341.

9. Claffy, E. W., C. C. Klick and F. H. Attix, "Thermoluminescent Process and Color Centers in LiF:Mg," Proceedings of the Second International Conference on Luminescence Dosimetry, ed. J. A. Auxier, et. al. (U.S. Atomic Energy Commission, 1968), 302.

10. Dobson, P. N. and A. A. Midkiff, "Explanation of Supralinearity in Thermoluminescence of LiF in Terms of the Interacting Track Model," Health Phys., 18, 571 (1970).

11. Spurny, Z., "Thermoluminescent Dosimetry," Atomic Energy Review, 3, 61 (1965).

12. Schayes, R., C. Brooke, I. Kozlowitz and M. Lheureux, "Thermoluminescent Properties of Natural Calcium Fluoride," Luminescence Dosimetry, ed. F. H. Attix, (U.S. Atomic Energy Commission, Division of Technical Information, Oak Ridge, Tennessee, 1967), 138.

13. TL Dosimetry System, Models TL-3B and TL-3C, Operation Manual, #S-316-MN, EG and G, Santa Barbara Division, 1966.

14. Alexander, A. J., "The Response Characteristics of CaF_2:Mn Thermoluminescent Dosimeters," M.S. Thesis, Kansas State University, 1970.

15. Smarsh, J. D., "Effects of Very High Dose Rates on the Response of Calcium Fluoride Thermoluminescent Dosimeters," M.S. Thesis, Kansas State University, 1971.

16. Morehead, F. F. and F. Daniels, "Thermoluminescence and coloration of LiF Produced by Alpha Particles, Electrons, Gamma Rays and Neutrons," J. Chem. Phys., 27, 1318 (1957).

17. Nash, A. E., F. H. Attix and J. H. Schulman, "Spurious Thermoluminescence of CaF_2:Mn and LiF (TLD-100)," Thermoluminesce Dosimetry, ed. F. H. Attix, (U.S. Atomic Energy Commission, Division of Technical Information, Oak Ridge, Tennessee, 1967), 244.

18. Kaiseruddin, M., "Effects of Very High Dose Rates of the Response of LiF Thermoluminescent Dosimeters," M.S. Thesis, Kansas State University, 1968.

19. Bliss, C. E., "The Response of ^{6}LiF and ^{7}LiF Thermoluminescent Dosimeters to Neutron and Gamma-Radiation Dose," M.S. Thesis, Kansas State University, 1972.

20. Prigel, D. W., "Neutron Spectra Measurements with miniature NE-213 Spectrometers," M.S. Thesis, Kansas State University, 1972.

21. Thiesing, J. W. and W. Meyer, "The Orders-of-Scattering Method for Fast Neutron Transport," U.S. Atomic Energy Commission Document No. COO-2049-90, August 25, 1971.

22. Californium-252 Progress, U.S. Atomic Energy Commission, Savannah River Laboratory, No. 8, July, 1971, 42.

12. APPENDICES

APPENDIX A

Data and Results for the Gamma Calibration Curve

Sample Number	Duration of irradiation, (min.)	Timed dose, (rad)	Total dose, (rad)	Response (reader units) $\bar{X}$	$\sigma_{\bar{X}}$	σ_X
1	0	0	102.36	2.86	0.2	0.824
2	0.3	643.14	745.50	21.2	0.72	2.968
3	0.6	1286.28	1388.64	39.5	1.55	6.390
4	0.9	1929.42	2031.78	55.5	2.31	9.524
5	1.2	2572.56	2674.92	70.20	4.0	16.491
6	1.5	3215.70	3318.06	92.0	2.9	11.956
7	1.8	3858.84	3961.20	117.0	2.7	11.132
8	2.1	4501.98	4606.34	132.0	6.4	26.38
9	2.4	5145.12	5247.48	144.0	5.88	24.23
10	3.0	6431.40	6533.76	167.0	6.2	25.56
11	3.5	7503.30	7605.66	203.0	5.07	20.90
12	4.0	8575.10	8677.59	223.0	7.91	32.61
13	4.5	9851.82	9749.46	253.0	9.83	40.52
14	5.0	10719.14	10821.50	279.0	10.0	41.23
15	5.5	11790.90	11893.26	327.0	11.6	47.82
16	6.0	12862.80	12965.16	386.0	9.30	38.34
17	6.5	13933.40	14035.76	408.0	12.0	49.47
18	7.0	15006.60	15108.96	418.0	14.0	57.72
19	9.0	19294.19	19396.55	549.0	20.3	83.69
20	10.0	21438.00	21540.35	587.0	21.0	86.58
21	11.0	23581.80	23684.16	712.0	22.0	90.70
22	13.0	27869.40	27971.76	911.0	23.0	94.82
23	15.0	32157.00	32259.35	1054.0	32.0	131.93
24	20.0	42876.00	42978.35	1365.0	60.0	247.38
25	30.0	64314.00	64416.36	2227.0	121.0	498.88
26	40.0	85752.00	85854.36	3353.0	118.0	486.51

Appendix A (cont'd)

27	60.0	128628.00	128730.36	3867.0	268.0	1104.96
28	80.0	171504.00	171606.36	5504.0	236.0	973.02
29	160.0	343008.00	343110.36	9648.0	236.0	973.02

Mean value $= \bar{X} = \frac{1}{N} \sum_{i=1}^{N} X_i$

Standard deviation of mean $= \sigma_{\bar{X}} = \left(\frac{\sum_{i=1}^{N} (X_i - \bar{X})^2}{N(N-1)} \right)^{1/2}$

Standard deviation of individual measurement $= \sigma_X = \left(\frac{\sum_{i=1}^{N} (X_i - \bar{X})^2}{N} \right)^{1/2}$

APPENDIX B

Data and Results for the Neutron Calibration Curve

Sample number	Duration of irradiation, (min.)	Fluence, (n/cm^2)	Response, (reader units) $\bar{X}$	$\sigma_{\bar{X}}$	σ_X
1	1.0	3.6×10^{10}	1.110	0.067	0.276
2	2.0	7.2×10^{10}	2.136	0.051	0.210
3	4.0	1.44×10^{11}	4.14	0.117	0.482
4	5.0	1.8×10^{11}	4.19	0.214	0.882
5	10.0	3.6×10^{11}	9.05	0.309	1.274
6	30.0	1.08×10^{12}	26.4	0.944	3.892
7	60.0	2.16×10^{12}	57.6	2.04	8.410
8	90.0	3.24×10^{12}	92.0	2.5	10.307
9	120.0	4.32×10^{12}	130.0	3.96	16.327
10	150.0	5.40×10^{12}	153.0	4.10	16.904
11	180.0	6.45×10^{12}	185.3	8.32	34.303
12	200.0	7.20×10^{12}	217.0	10.0	41.230
13	220.0	7.92×10^{12}	245.0	10.0	41.230
14	240.0	8.64×10^{12}	272.0	9.4	38.756
15	270.0	9.72×10^{12}	310.0	9.63	39.704
16	300.0	1.08×10^{12}	352.0	14.0	57.721
17	330.0	1.188×10^{13}	397.0	14.7	60.608
18	360.0	1.296×10^{13}	428.0	12.3	50.712
19	390.0	1.404×10^{13}	468.0	11.7	48.239
20	427.0	1.538×10^{13}	515.0	20.0	82.45
21	450.0	1.62×10^{13}	540.0	12.9	53.18

APPENDIX B (cont'd)

22	480.0	1.728×10^{13}	583.0	24.0	98.95
23	510.0	1.836×10^{13}	603.0	17.5	72.15
24	560.0	2.016×10^{13}	692.0	15.8	65.14
25	600.0	2.16×10^{13}	731.0	20.0	82.45
26	700.0	2.52×10^{13}	880.0	30.0	123.69
27	800.0	2.88×10^{13}	1015.0	39.0	160.79
28	900.0	3.24×10^{13}	1150.0	60.0	247.38
29	1000.0	3.6×10^{13}	1244.0	46.0	189.65
30	1200.0	4.32×10^{13}	1498.0	69.0	284.48
31	1350.0	4.86×10^{13}	1745.0	65.0	267.99
32	1500.0	5.4×10^{13}	1837.0	60.0	247.38
33	2000.0	7.2×10^{13}	2582.0	87.0	358.70
34	2500.0	9.0×10^{13}	3196.0	123.0	507.12
35	3000.0	1.08×10^{14}	4054.0	190.0	783.36
36	5000.0	1.8×10^{14}	6042.0	234.0	964.78

Mean value = $\bar{X} = \frac{1}{N} \sum_{i=1}^{N} X_i$

Standard deviation of mean = $\sigma_{\bar{X}} = \left(\frac{\sum_{i=1}^{N} (X_i - \bar{X})^2}{N(N-1)} \right)^{1/2}$

Standard deviation of individual measurement = $\sigma_X = \left(\frac{\sum_{i=1}^{N} (X_i - \bar{X})^2}{N} \right)^{1/2}$

THE RESPONSE OF CaF_2:Mn THERMOLUMINESCENT DOSIMETERS TO NEUTRONS FROM A ^{252}Cf SOURCE

by

CHI-GEE KAN

B.S., National Tsing Hua University
Republic of China, 1969

AN ABSTRACT OF A MASTER'S THESIS

submitted in partial fulfillment of the

requirements for the degree

MASTER OF SCIENCE

Department of Nuclear Engineering

KANSAS STATE UNIVERSITY
Manhattan, Kansas

1973

ABSTRACT

The theory of thermoluminescence and pertinent thermoluminescent dosimetry for the EG and G model TL-39 CaF_2:Mn Microthermoluminescent Dosimeters were briefly reviewed. A calibration curve for the TL-39 dosimeters was experimentally determined with ^{60}Co gamma ray for the dose of 100 to 3 x 10^5 rad.

To obtain the fission neutron source the ^{252}Cf facility at Kansas State University was used. Two kinds of estimation to the absolute fast-neutron flux in the center of the ^{252}Cf sources has been done in this study. A fast-neutron flux of 6.0 x 10^9 neutron/cm^2sec was used to irradiate the dosimeter. A calibration curve for the TL-39 dosimeters was experimentally determined for the fast-neutron fluences of 3.6 x 10^{10} to 1.8 x 10^{14} neutrons/cm^2.

Data were analyzed by a least-square method. The conclusions drawn were: (1) The response of CaF_2:Mn to the neutrons from ^{252}Cf is not linear; the supralinearity occurs between the fast-neutron fluence of 7.2 x 10^{12} and 7.92 x 10^{12} neutron/cm^2. (2) The slope of the intermediate fluence range in the calibration curve is 1.305 times the slope in the low fluence range. (3) The saturation region in the neutron calibration curve starts at approximately 1.8 x 10^{14} neutrons/cm^2.